AFRL-AFOSR-VA-TR-2016-0354

High-Energy, Multi-Octave-Spanning Mid-IR Sources via Adiabatic Difference Frequency Generation

Franz Kaertner
MASSACHUSETTS INSTITUTE OF TECHNOLOGY

10/17/2016
Final Report

DISTRIBUTION A: Distribution approved for public release.

Air Force Research Laboratory
AF Office Of Scientific Research (AFOSR)/ RTB1
Arlington, Virginia 22203
Air Force Materiel Command

REPORT DOCUMENTATION PAGE

Form Approved
OMB No. 0704-0188

The public reporting burden for this collection of information is estimated to average 1 hour per response, including the time for reviewing instructions, searching existing data sources, gathering and maintaining the data needed, and completing and reviewing the collection of information. Send comments regarding this burden estimate or any other aspect of this collection of information, including suggestions for reducing the burden, to Department of Defense, Executive Services, Directorate (0704-0188). Respondents should be aware that notwithstanding any other provision of law, no person shall be subject to any penalty for failing to comply with a collection of information if it does not display a currently valid OMB control number.
PLEASE DO NOT RETURN YOUR FORM TO THE ABOVE ORGANIZATION.

1. REPORT DATE *(DD-MM-YYYY)*	2. REPORT TYPE	3. DATES COVERED *(From - To)*
08-11-2016	Final Performance	15 Mar 2013 to 14 Jul 2016

4. TITLE AND SUBTITLE
High-Energy, Multi-Octave-Spanning Mid-IR Sources via Adiabatic Difference Frequency Generation

5a. CONTRACT NUMBER

5b. GRANT NUMBER
FA9550-13-1-0159

5c. PROGRAM ELEMENT NUMBER
61102F

6. AUTHOR(S)
Franz Kaertner, Jeffery Moses

5d. PROJECT NUMBER

5e. TASK NUMBER

5f. WORK UNIT NUMBER

7. PERFORMING ORGANIZATION NAME(S) AND ADDRESS(ES)
MASSACHUSETTS INSTITUTE OF TECHNOLOGY
77 MASSACHUSETTS AVE
CAMBRIDGE, MA 02139-4301 US

8. PERFORMING ORGANIZATION REPORT NUMBER

9. SPONSORING/MONITORING AGENCY NAME(S) AND ADDRESS(ES)
AF Office of Scientific Research
875 N. Randolph St. Room 3112
Arlington, VA 22203

10. SPONSOR/MONITOR'S ACRONYM(S)
AFRL/AFOSR RTB1

11. SPONSOR/MONITOR'S REPORT NUMBER(S)
AFRL-AFOSR-VA-TR-2016-0354

12. DISTRIBUTION/AVAILABILITY STATEMENT
A DISTRIBUTION UNLIMITED: PB Public Release

13. SUPPLEMENTARY NOTES

14. ABSTRACT

The creation of energetic, arbitrarily shapeable, multi-octave-spanning, coherent sources of short-wave, mid-wave, and long-wave mid-IR light is valuable to many independent fields of research and technology development, from detection of ultrafast energy transfer in proteins and biological molecules across functional groups, to high-flux, table-top generation of coherent keV photons, time-resolved tomography of molecular orbital structure, and coherent control of vibrational dynamics of molecules. And it could further applications as diverse as laser ablation of polymers, infrared countermeasures for defense, laser ranging, and compact electron beam acceleration.
Under this grant, we have achieved the main goals of our research plan. We have evaluated a brand-new concept in nonlinear optics, adiabatic difference frequency generation (ADFG) for the efficient transfer of broadband, high-energy near-IR lasers to the mid-IR, allowing the generation of high-energy, multi-octavespanning, short- and mid-wave IR pulsed sources in the 2-5 m range and demonstration of compressed single-cycle mid-IR pulses. Adiabatic frequency conversion applies the concept of robust population transfer by rapid adiabatic passage to nonlinear optical frequency conversion. The concept effectively avoids two main hurdles of optical frequency generation: limited bandwidth and limited conversion efficiency.

15. SUBJECT TERMS

DISTRIBUTION A: Distribution approved for public release.

16. SECURITY CLASSIFICATION OF:			17. LIMITATION OF ABSTRACT	18. NUMBER OF PAGES	19a. NAME OF RESPONSIBLE PERSON
a. REPORT	b. ABSTRACT	c. THIS PAGE			PARRA, ENRIQUE
Unclassified	Unclassified	Unclassified	UU		19b. TELEPHONE NUMBER *(Include area code)* 703-696-8571

DISTRIBUTION A: Distribution approved for public release.

FINAL PROGRESS SUMMARY

To: technicalreports@afosr.af.mil

Subject: Final Progress Statement to Dr. Enrique Parra

Contract/Grant Title: (YIP) High-Energy, Multi-Octave-Spanning Mid-IR Sources via Adiabatic Difference Frequency Generation

Contract/Grant #: FA9550-13-1-0159

Reporting Period: 15 March 2013 to 14 July 2016

Abstract

The creation of energetic, arbitrarily shapeable, multi-octave-spanning, coherent sources of short-wave, mid-wave, and long-wave mid-IR light is valuable to many independent fields of research and technology development, from detection of ultrafast energy transfer in proteins and biological molecules across functional groups, to high-flux, table-top generation of coherent keV photons, time-resolved tomography of molecular orbital structure, and coherent control of vibrational dynamics of molecules. And it could further applications as diverse as laser ablation of polymers, infrared countermeasures for defense, laser ranging, and compact electron beam acceleration.

Under this grant, we have achieved the main goals of our research plan. We have evaluated a brand-new concept in nonlinear optics, adiabatic difference frequency generation (ADFG) for the efficient transfer of broadband, high-energy near-IR lasers to the mid-IR, allowing the generation of high-energy, multi-octave-spanning, short- and mid-wave IR pulsed sources in the 2-5 μm range and demonstration of compressed single-cycle mid-IR pulses. Adiabatic frequency conversion applies the concept of robust population transfer by rapid adiabatic passage to nonlinear optical frequency conversion. The concept effectively avoids two main hurdles of optical frequency generation: limited bandwidth and limited conversion efficiency.

Moreover, we have shown that our ADFG technique is particularly convenient for the low-cost extension to the mid-IR of existing ultrafast laser architectures in the near-IR, requiring the addition of only a single nonlinear conversion stage based on an aperiodically poled quasi-phase-matching grating. Thus, a broadband source built on conventional laser technology can be immediately extended to the mid-IR, thus saving a research facility the considerable expense of a new laser system built to span a mid-IR frequency range. In our work, we have shown how the addition of a single adiabatic conversion stage to a conventional noncollinear, near-IR optical parametric chirped pulse amplification (OPCPA) system, can produce a multi-octave spanning mid-IR source emitting single-cycle and arbitrarily shaped mid-IR pulses. Additionally, we have shown that the ADFG mid-IR pulses can be used conveniently as the seed source for an octave-spanning mid-IR OPCPA pumped by 2-micron wavelength pulses.

Furthermore, we have experimentally verified that ADFG transfers the spectral phase and amplitude profile of the near-IR pulse to the mid-IR pulse with a linear transfer function, and its conversion efficiency does not depend on the initial phase and amplitude of the near-IR pulse. This “one-to-one” conversion dynamic allows a pulse to be modulated in the near-IR by existing pulse-shaping techniques, and desired phase and amplitude properties of the octave-spanning

DISTRIBUTION A: Distribution approved for public release.

mid-IR pulse can be obtained without the photon losses or dollar costs for shaping technologies in the mid-IR spectral range.

Importantly, this means that the ADFG approach, including a conventional sub-octave near-IR pulse shaper (such as an acousto-optic programmable dispersive filter (AOPDF) or 4f-pulse shaper), can be used as a *multi-octave* mid-IR pulse shaper. We have demonstrated such a technology for the first time.

Finally, we advanced the approach towards future directions. Through modeling of ultrabroadband ADFG pulse propagation we have identified an analytical formula capturing the dispersion of the ADFG device. We have evaluated and modeled the extension of the ADFG approach to the long-wave IR through the use of orientation patterned semiconductors. And we have developed a scheme for employing the ADFG approach in a multi-spectral spectroscopy system providing 10-fs pulses in many ranges of the electromagnetic spectrum.

List of milestones reached

1) **Design of octave-spanning mid-IR conversion grating.** Designed an adiabatically chirped quasi-phase matching grating for simultaneous phase-matching of difference frequencies spanning the near-IR and mid-IR, from 1.3-6 microns.
2) **Design of a near-IR to mid-IR high energy conversion system architecture based on OPCPA and ADFG.** Modified an 800-nm OPCPA to produce 30-microjoule seed pulses spanning from 690-890 nm wavelengths, corresponding to 2.0-6.0 micron difference frequencies when mixed with a 1047-nm pump pulse, and implemented this as the seed pulse for an ADFG-based mid-IR conversion stage. With this design, the mid-IR source is simply a standard near-IR OPCPA with a single ADFG conversion stage added at the end.
3) **Demonstration of octave-spanning mid-IR generation.** Demonstrated generation of a coherent, 1.1-octave spectrum spanning from 2.1-4.7 microns at -10 dB from the peak (thus displaying unprecedented flatness of power spectrum for a mid-IR continuum), with microjoule energy. The full bandwidth spanned from 2.0-5.5 microns.
4) **Demonstration of octave-spanning amplitude shaping.** Confirmed the linear relationship of input to output power spectral profile. A near-IR pulse shaper implemented prior to the conversion stage was used to shape the spectrum of the generated mid-IR spectrum, thus demonstrating a highly convenient capability for multi-octave amplitude shaping.
5) **Pulse compression; Demonstration of a few-cycle, tunable mid-IR source.** By implementing a dispersion management system consisting of an acousto-optic programmable dispersive filter (AOPDF) prior to the conversion stage and a highly efficient anti-reflection-coated bulk silicon block compressor after the conversion stage, we achieved tunable compressed mid-IR pulses spanning 2-4 microns with 4-cycle pulse durations.
6) **Modeling of propagation effects and determination of the dispersion function.** We demonstrated pulse propagation simulations for modeling the adiabatic frequency conversion process, and determined an analytic function for the dispersion profile of the

DISTRIBUTION A: Distribution approved for public release.

ADFG process. This result confirmed the capability of ADFG to provide a linear transfer function of phase profile from near-IR to mid-IR across the full bandwidth, a key development for achieving transform limited pulse compression of the multi-octave bandwidth in our experiments.

7) **Generation of single-cycle mid-IR pulses.** Achieved single-cycle, transform limited pulse duration. We measured a 1.2-optical cycle pulse at 2.6-micron wavelength (measuring 10.7 fs) generated by adiabatic frequency conversion using our home-built FROG characterization tool. This pulse spans from 1.8 – 4.5 microns at -10 dB from peak. To achieve this, we refined both our approach to dispersion control, programming our pulse shaper with an arbitrary phase function rather than a simple polynomial expansion, and our FROG device, increasing its acceptance bandwidth to 1.8 – 5 microns by use of a 30-micron GaSe crystal and by employing the marginal correction to achieve a reconstructed pulse covering the full spectral width of the real pulse.

8) **Demonstration of arbitrary, multi-octave pulse shaping.** Demonstrated arbitrary, multi-octave-spanning pulse shaping in the mid-IR. We used this approach to create, e.g., interferometrically stable, single-cycle, mid-IR pulse pairs of arbitrary spacing, as might be used for multidimensional spectroscopy.

9) **Implementation as a seed pulse for ultrabroadband mid-IR OPA.** We demonstrated the use of the octave-spanning ADFG pulse as a seed pulse for optical parametric amplification with a 2-micron-wavelength pump pulse, producing an amplified idler pulse at 6-micron wavelength with a compressed duration of 34 fs (1.7 optical cycles).

10) **Modeling and design of extended long-wave-IR source.** Employing our propagation simulations, we designed an extension of the frequency conversion technique to cover the thermal infrared along the 5-12 micron wavelength range using orientation poled gallium phosphide.

11) **Design of multi-spectral, 10-fs spectroscopy system based on ADFG.** We have developed a system architecture employing the ADFG approach in order to build a multi-spectral spectroscopy system at Cornell providing 10-fs pulses in many ranges of the electromagnetic spectrum.

Archival publications during reporting period:

1. H. Suchowski, P. R. Krogen, S.-W. Huang, F. X. Kärtner, and J. Moses, "Octave-spanning coherent mid-IR generation via adiabatic difference frequency conversion," Opt. Express **21**, 28892-28901 (2013).

2. K.-H. Hong, C.-J. Lai, J. Siqueira, P. Krogen, J. Moses, L. C.-L. Chang, G. J. Stein, L. E. Zapata, and F. X. Kärtner "Multi-mJ, kHz, 2.1-μm optical parametric chirped-pulse amplifier and high-flux soft X-ray high-harmonic generation," Opt. Lett. 39, 3145 (2014).

3. C. Manzoni, O. D. Mücke, G. Cirmi, S. Fang, J. Moses, S.-W. Huang, K.-H. Hong, G. Cerullo, and F. X. Kärtner, "Coherent pulse synthesis: towards sub-cycle optical waveforms," Laser & Photon. Rev. 9, 129 (2015).

DISTRIBUTION A: Distribution approved for public release.

4. C.-L. Chang, P. Krogen, H. Liang, G. J. Stein, J. Moses, C.-J. Lai, J. P. Siqueira, L. E. Zapata, F. X. Kärtner, and K.-H. Hong, "Multi-mJ, kHz, ps deep-ultraviolet source," Opt. Lett. 40, 665 (2015).

5. C.-L. Chang, P. Krogen, K.-H. Hong, L. E. Zapata, J. Moses, A.-L. Calendron, H. Liang, C.-J. Lai, G. J. Stein, P. D. Keathley, G. Laurent, and F. X. Kärtner, "High-energy, kHz, picosecond hybrid Yb-doped chirped-pulse amplifier," Opt. Express 23, 10132 (2015).

6. C.-J. Lai, K.-H. Hong, J. P. Siqueira, P. Krogen, C.-L. Chang, G. J. Stein, H. Liang, P. D. Keathley, G. Laurent, J. Moses, L. E. Zapata, and F. X. Kärtner, "Multi-mJ mid-infrared kHz OPCPA and Yb-doped pump lasers for tabletop coherent soft x-ray generation," J. Opt. 17, 094009 (2015).

7. C. Manzoni, O. D. Mücke, G. Cirmi, S. Fang, J. Moses, S.-W. Huang, K.-H. Hong, G. Cerullo, and F. X. Kärtner, "Coherent pulse synthesis: towards sub-cycle optical waveforms," Laser & Photon. Rev. 9, 129 (2015).

Conference papers during the reporting period, not yet published in archival journals:

1. P. Krogen, H. Suchowski, G. J. Stein, F. Kärtner, and J. Moses, "Tunable and Near-Fourier-limited Few-Cycle Mid-IR Pulses via an Adiabatically Chirped Difference Frequency Grating," in CLEO: 2014, OSA Technical Digest (online) (Optical Society of America, 2014), paper SM3I.5.

2. P. R. Krogen, H. Suchowski, G. J. Stein, F. X. Kärtner, and J. Moses, "Tunable Few-Cycle Mid-IR Pulses towards Single-Cycle Duration by Adiabatic Frequency Conversion," in 19th International Conference on Ultrafast Phenomena, OSA Technical Digest (online) (Optical Society of America, 2014), paper 08.Tue.D.6.

3. P. Krogen, H. Suchowski, H. Liang, F. X. Kaertner, and J. Moses, "Toward Multi-Octave Pulse Shaping by Adiabatic Frequency Conversion," in CLEO: 2015, OSA Technical Digest (online) (Optical Society of America, 2015), paper SW1O.3.

4. P. Krogen, H. Suchowski, H. Liang, K.-H. Hong, F. Kärtner, J. Moses, "Generation of a Single-Cycle Pulse at 2.6 μm using Adiabatic Difference Frequency Generation," in International Conference on Ultrafast Phenomena, OSA Technical Digest (online) (Optical Society of America, 2016), paper UTu2A.1.

5. H. K. Liang, P. Krogen, K. Zawilski, P. G. Schunemann, T. Lang, U. Morgner, F. Kärtner, J. Moses, and K. Hong, "Octave-Spanning 6-μm OPA Pumped by 2.1-μm OPCPA," in High-Brightness Sources and Light-Driven Interactions, OSA technical Digest (online) (Optical Society of America, 2016), paper MS4C.1.

6. P. Krogen, H. K. Liang, K. Zawilski, P. G. Schunemann, T. Lang, U. Morgner, J. Moses, F. Kärtner, and K. Hong, "Octave-spanning 1.5-optical-cycle 6.5-μm OPA pumped by 2.1-μm OPCPA," in Conference on Lasers and Electro-Optics, OSA Technical Digest (2016) (Optical Society of America, 2016), paper STu3I.4.

DISTRIBUTION A: Distribution approved for public release.

Details of milestones reached

1) **Design of octave-spanning mid-IR conversion grating.** [1]

Prior to the grant period, the broadest conversion achieved using ADFG employed an aperiodically poled KTP crystal of 2-cm length [2]. In this prior work done by our group, we measured 1-to-1 photon conversion from a broad Ti:sapphire oscillator band to the IR, using a 1.047-μm pump laser of 2 GW/cm^2 intensity. From the selected 625-740 nm visible/near-IR band, a 0.7-octave IR band covering 1.55 to 2.4 μm was generated. The DFG bandwidth was limited on the low-wavelength side by the finite bandwidth of the Ti:sapphire oscillator pulses, but on the long wavelength side, the conversion band was limited by the transmission window of KTP (absorbing above 2.5 μm).

In this grant program, using the quasi-phase matching (QPM) technique, we have designed an adiabatic aperiodically poled grating in a magnesium-oxide-doped congruent lithium niobate (MgCLN) nonlinear crystal. The poling satisfies the constraints imposed by the adiabatic inequality and the LZ prediction for adiabatic conversion [3], for a signal range of 600 to 870 nm, mixed with a 1047-nm strong narrowband pump, producing an idler range of 1405 to 5500 nm. We chose to use MgCLN nonlinear crystal for its wide spectral transparency window in the mid-IR and high damage threshold. In our simulation, we have used the Sellmeier coefficients retrieved from Ref. [4]. Although those coefficients were examined only up to wavelength of 4 μm, we have used them to calculate the adiabatic evolution even for higher wavelengths, exceeding 5 μm. In order to induce an adiabatic longitudinal change of the effective total phase mismatch parameter, defined as $\Delta k(z) = k_2 + k_3 - k_1 - G(z)$, we chose the function $G(z) = 990z^2 + 2400z + 4050$ [1/cm], where z (in cm) is measured from the center of the crystal (i.e., z varied from -1 cm to 1 cm). This design optimized, across signal frequencies, the uniformity of the adiabatic conversion rate, and has a QPM period, $\Lambda(z) = 2\pi/G(z)$, ranging from 8.4 to 23.8 μm.

Numerical finite-difference simulations of the design for a pump intensity of 8.1 GW/cm^2 (when assuming an average effective second order susceptibility of $d_{33}(\lambda)$ = 21.5 pm/V – a modified value for a DFG process using a Miller's rule prediction for MgCLN [5]), are shown in Fig. 1. The two-dimensional image shows the conversion efficiency as a function of the propagation length (x-axis) and for a broad output wavelength span covering 1100 nm to 6400 nm (y-axis). In order to better perceive the information, we have plotted in the upper figure several horizontal cross sections of different wavelengths (1500, 2000, 2500, 3000, 4250, 5500 and 6400 nm), showing the adiabatic evolution of those waves. As seen, each signal is adiabatically converted at a different location in the nonlinear crystal.

As can be seen, at the output facet of the nonlinear crystal the predicted photon number conversion efficiency is very high (above 80% for I_2> 8.1 GW/cm2 for an idler range of 1.4 to 5.5 μm). These values are in very good agreement with the use of the Landau-Zener formula. Note, these simulations neglect the linear absorption of MgCLN, which can be expected to result in a significant reduction in efficiency above 5-μm wavelength. It is also worth noting that due to lack of literature data on MgCLN for those long wavelengths, we assume in our numerical simulations that the nonlinear susceptibility is constant for the entire spectral range.

DISTRIBUTION A: Distribution approved for public release.

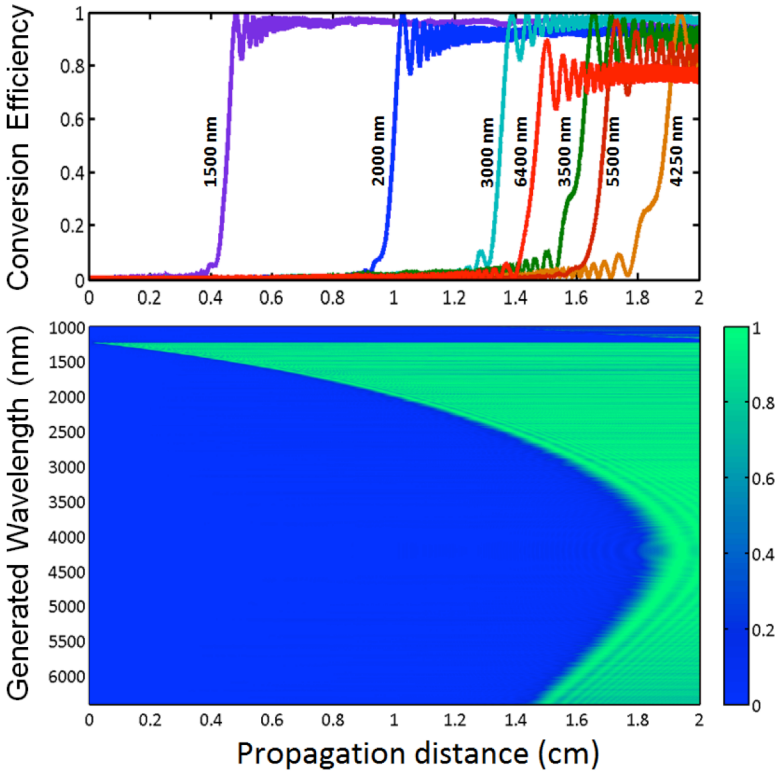

Fig. 1. (From [1]) The octave-spanning adiabatic difference frequency design. Main figure: two-dimensional map of the conversion efficiency as a function of generated wavelength (y-axis) and the location along the adiabatic aperiodically poled nonlinear crystal (x-axis). The pump intensity is 8.1 GW/cm^2. The upper panel shows the conversion efficiency for several wavelengths along the propagation axis. As seen, all are designed to have adiabatic trajectories for efficient conversion from near IR to mid IR. At the output facet of the nonlinear crystal (L = 2 cm), high conversion efficiency is achieved for the 1300-5500 nm spectral range.

2) **Design of a near-IR to mid-IR high energy conversion system architecture based on OPCPA and ADFG.** [1]

The experimental system we designed to test the multi-octave ADFG frequency converter consisted of a combination of a near-IR OPCPA and an adiabatic difference frequency generation (ADFG) stage, illustrated in Fig. 2. This system represents a very simple extension of a near-IR OPCPA system to octave-spanning mid-IR, requiring nothing other in addition than a single aperiodically poled MgCLN crystal. A Ti:sapphire oscillator injection seeds a Nd:YLF chirped pulse amplifier (CPA), and a 2-stage parametric amplifier. The Nd:YLF CPA is home-built and delivers 12-ps, 1-kHz, 4-mJ pulses at 1047nm [6], which are then used to pump the OPCPA after second harmonic generation (SHG) in a 10-mm-long noncritically phase-matched LBO crystal, and to pump the ADFG process. The near-IR signal pulse source is a modified OPCPA system that delivers 1-kHz, ~4 ps chirped pulses spanning 0.7-0.9 μm with up to 20-μJ energy. In the experiment, these pulses were combined collinearly at a dichroic mirror (DM) with up to ~0.5 mJ of the remaining Nd:YLF pulse energy at 1047 nm and sent to the aperiodically poled MgCLN grating described in Section 1 for broadband ADFG, with telescopes employed to keep the chirped broadband near-IR beam (*i.e.*, the ADFG "signal")

DISTRIBUTION A: Distribution approved for public release.

smaller than one-half the size of the 1047-nm beam (*i.e.*, the ADFG "pump"). The MgCLN grating has an aperture of 1 mm x 3 mm.

The OPCPA (Fig. 2, bottom) is capable of delivering 30-μJ, 8-fs, 1-kHz pulses with a bandwidth covering 0.69-1.05μm, and was modified for this application by diverting the amplified beam before the glass compressor normally used to dechirp the pulses, and by narrowing the gain bandwidth to match the 0.69-0.87 μm range desired for later adiabatic conversion. The modified configuration uses 1 or 2 noncollinear optical parametric amplifier (NOPA) stages in BBO, and a combination of grism pairs, dispersive glass, and an acousto-optic programmable dispersive filter (Dazzler, Fastlite) to control the dispersion throughout the experiment. The first NOPA stage consists of a 5-mm thick BBO crystal cut at θ=24.0° with a noncollinear angle α=2.4°, pumped by 500-μJ pulses at 523 nm, an energy optimized for a gain of ~10^5 to amplify the weak Ti:sapphire oscillator pulses to ~1-μJ. These are then further amplified in another NOPA, which consists of a 3-mm thick BBO, again with θ=24.0°, α=2.4°, pumped by 600-μJ pulses at 523nm, resulting in a gain of ~10^3 which compensates for the losses in the dispersive elements between stages, and gives the final output energy of 20 μJ with a clean spatial profile.

Careful considerations were made in regards to the chirp in the NOPA system to ensure that there is a good temporal overlap between the pump and seed in both the NOPA stages and in the ADFG process. The Ti:sapphire seed pulses were first stretched to 2.5 ps in a grism pair with a group velocity dispersion (GVD) of -6300 fs^2, optimized to overlap with the 8-ps NOPA pump pulses for efficient amplification in the 0.69-0.87-μm range in the first NOPA stage. The pulses were then further stretched by a grism+Dazzler combination providing an additional -4000 fs^2 of GVD to stretch the pulse to 3.7 ps. Conveniently, this duration (3.7 ps) was also appropriate for the ADFG stage, allowing good overlap with the 12-ps pump duration. Additionally, the 3.7-ps duration was long enough to prevent significant group velocity walkoff between the interacting pulses and compression of the signal pulses due to the normal dispersion of MgCLN at near-IR wavelengths. The mid-IR power was collected by a scanning monochromator with a thermo-electrically cooled PbSe photodetector (Horiba/JY). The relative spectral intensity response of the monochromator and photodetector were calibrated with a temperature-controlled black-body source. A Ge order-sorting filter was used to block any residual NIR leakage.

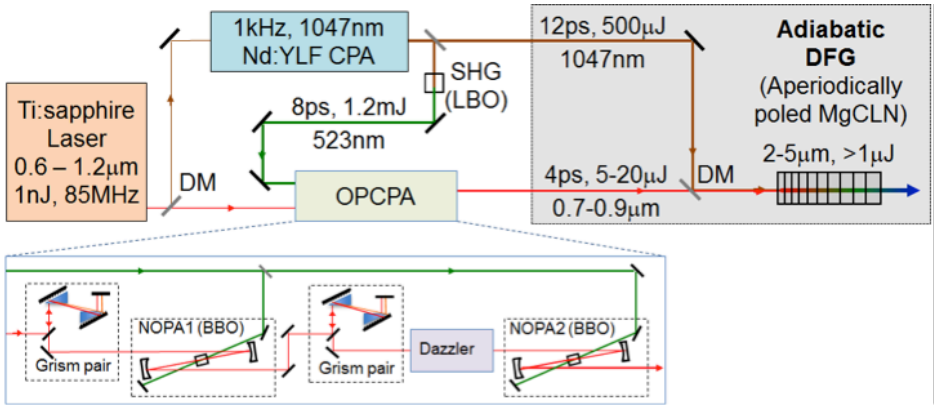

Fig. 2. (From [1]) Experimental setup for adiabatic difference frequency conversion of OPCPA pulses (top) and detail of the OPCPA system (bottom).

3) **Demonstration of octave-spanning mid-IR generation.** [1]

The experimental validation of the octave-spanning downconversion consisted of several sets of experiments. By using various broadband OPCPA input pulses with variable spectral profiles, we could verify the response of the conversion device and demonstrate its applicability for accurate conversion of broadband near-IR pulses. The main result of this study was an exceptionally flat and greater-than-octave spanning mid-IR spectrum, spanning 2.1-4.7 μm, or 1.1 octaves, at -10 dB of peak.

Figure 3 shows the normalized measured power spectrum (solid curve) of a generated mid-IR pulse alongside the normalized "expected" power spectral density (dashed black curve) calculated by assuming 100% conversion of the OPCPA power spectrum to the mid-IR via ADFG and accounting for the varying quantum defect, $\lambda_{signal}/\lambda_{idler}$. We observe a clear transfer of the spectral amplitude profile from near-IR to mid-IR, resulting in observable power spectral density on a linear scale from 2-5 μm. At -10 dB of peak, the spectrum spans 2.1-4.7 μm, or 1.1 octaves $= \log_2[4.7\mu m/2.1\mu m]$. The maximum mid-IR pulse energy we obtained is 1.5 μJ, equivalent to an 83% internal photon number conversion of the 7.9 μJ of OPCPA pulse energy in the incident 680-870-nm range (see inset), once we have accounted for the 23% quantum efficiency integrated over the spectrum. This is slightly lower than the expected ~90% internal photon number conversion efficiency expected from our simulations. The small discrepancies between expected and measured power spectra are under current investigation, and are likely due to ambient absorption, QPM grating manufacturing errors, and/or linear absorption in the MgCLN crystal at long wavelengths. We note that we observed by eye a small amount of green and violet light emanating from the lithium niobate grating, indicating some parasitic second harmonic generation of the pump and signal waves. The pump loss appeared negligibly small, but the signal loss could account for the few-percent discrepancy between expected and measured mid-IR power. Generally, these processes are not directly phase-matched by first-order QPM in our design, so do we not expect them to be limiting, but this could plausibly be a limitation for designs requiring a significantly higher pump or signal intensity.

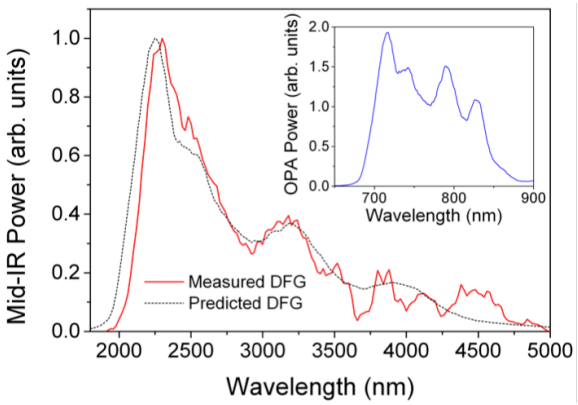

Fig. 3. (From [1]) Octave-spanning mid-IR spectrum. The red solid curve is the experimental spectrum, while the dashed black line is the normalized expected spectrum, assuming a100% photon number conversion efficiency. Inset: the inputted near-IR spectrum from the OPCPA.

The mid-IR beam was imaged using a pyroelectric array imager, and displayed a nearly Gaussian profile with an ellipticity of 1.2, comparable to the ellipticity of the input near-IR beam, which had an ellipticity of 1.1. We note that the ellipticity of the mid-IR beam depended critically on the alignment, increasing as we misaligned the system by introducing a non-

DISTRIBUTION A: Distribution approved for public release.

collinear angle between the pump and signal beams. To test the frequency dependence of the mid-IR beam profile, we used the AOPDF to select portions of the input near-IR spectrum spanning roughly one-third of the full spectral width. The resulting portions of the mid-IR spectrum after conversion showed no significant variation in beam size, shape or location.

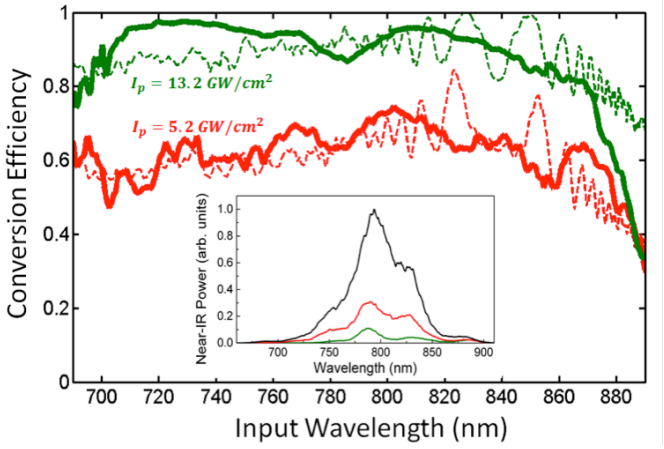

Fig. 4. (From [1]) Conversion efficiency (solid curves), following Eq. 1, retrieved from the experimentally observed depletion of the near-IR power spectra as a function of pump intensity. The simulated conversion efficiencies at the output facet of the nonlinear crystal are also plotted (dashed lines), using values of the pump intensity a factor of 1.6 lower than the two experimental values, respectively. The measured near-IR spectral power densities are shown explicitly in the inset, where black, red and green curves are for pump intensities of 0, 5.2 and 13.2 GW/cm^2, respectively. The numerical predictions and the measured conversion efficiencies are in very good agreement for spectral components as high as 870 nm (which corresponds to 5500 nm).

In order to further examine the adiabatic difference frequency converter, we have measured not only the generated signal in the mid-IR regime, but also the depletion of the incoming near-IR OPCPA pulses, and from this we have analyzed the implied conversion efficiency. The measured near-IR spectral power densities can be seen explicitly in the inset of Fig. 4, where black, red and green curves are for pump intensities of 0 GW/cm^2, 5.2 GW/cm^2, and 13.2 GW/cm^2, respectively. To calculate the implied conversion efficiency for each spectral component, we have used the following relation:

$$\eta(\lambda) = \frac{P_0(\lambda) - P_{I_p}(\lambda)}{P_0(\lambda)}, \qquad (1)$$

Where P_{Ip} is the spectral power density for a specific pump power I_p, and P_0 is the undepleted near-IR spectrum (where the narrowband pump was not used, and thus, I_p=0). Figure 4 shows the resulting implied conversion efficiencies obtained from the near-IR spectral depletion and Eq. 1 (solid red and black curves for the two pump intensities, respectively), alongside the simulated conversion efficiency as a function of the input wavelengths for two pump intensities, 3.2 GW/cm^2 and 8.1 GW/cm^2 (dashed blue and gray curves for the two pump intensities, respectively). As seen, though the simulated pump intensity values differ from each of the respective experimental values by a factor of 1.6, the numerical predictions of the conversion efficiency for both of the pump intensities are in very good agreement with the retrieved conversion efficiency. This is true for spectral components of the near-IR field as high as 870 nm (which corresponds to 5500 nm in the mid IR). Also, the good agreement of the conversion efficiency between 4000-6000 nm expands the literature values for MgCLN nonlinear crystal beyond the reported values examined in [4]. The factor of 1.6 can be explained partially by the

fact that the average experimental pump intensity overlapped with the near-IR pulse is lower than the corresponding peak intensity. It might also be explained by the fact that in our numerical simulations, we have assumed an average nonlinear susceptibility of $d_{33}(\lambda) = 21.5$ pm/V for the entire spectral range, which is an estimated average value of the effective nonlinear susceptibility using the Miller's rule prediction for the DFG process. In the mid-IR, this value varies from $d_{33}(\lambda_s = 690\text{ nm}, \omega_p = 1047\text{ nm}; \omega_i = 2025\text{ nm}) \approx 24$ pm/V to $d_{33}(\lambda_s = 900\text{ nm}, \omega_p = 1047\text{ nm}; \omega_i = 6400\text{ nm}) \approx 19$ pm/V, where we took Miller's delta to be $\Delta_{miller} = 16$ pm/V. The true value might be even lower, due to the fact that the experimental verification of the 2nd-order susceptibility has been shown to have a deviation from Miller's rule [5]. As shown before, the coupling coefficient between the interacting waves is proportional to $\kappa \propto d_{eff}^2 I_2$, meaning that an inaccurate value of d_{33} will have a strong impact. Note, the data presented in Fig. 4 also confirms the insensitivity of the adiabatic conversion rate to the signal intensity, as we see a flat conversion efficiency over a wavelength range including near-IR power spectral densities as low as -10dB relative to the peak.

4) **Demonstration of octave-spanning amplitude shaping.** [1]

Since an adiabatic difference frequency converter preserves the absolute bandwidth of a pulse while expanding its relative bandwidth, if it can also transfer the spectral amplitude profile from near-IR to mid-IR, then it can serve as multi-octave pulse shaper. A necessary step in establishing this capability is to confirm the linear relationship of input to output power spectral profile of an adiabatic frequency conversion process.

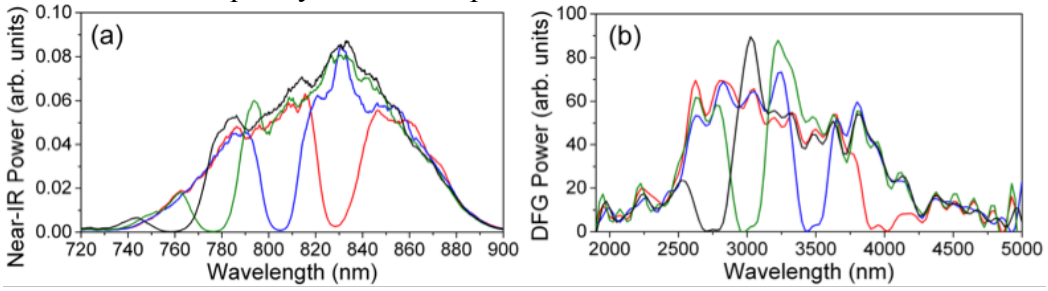

Fig. 5. (From [1]) Efficient and robust conversion of amplitude-shaped spectra. (a) Various OPCPA near-IR pulses that were shaped by a Dazzler in order to eliminate certain wavelength components in their spectral power densities. (b) The converted mid-IR spectra. As seen, one-to-one correspondence of the spectral hole locations and widths is achieved for all spectra.

To do this, we examined the expected flatness of the conversion response. With the Dazzler acoustic pulse shaper that we have in the OPCPA apparatus (see Fig. 2), spectral holes were created in the near-IR spectral power densities. These can be seen in Fig. 5(a). The black, green, blue and red curves correspond to near-IR spectra with spectral holes inserted at 760 nm, 777 nm, 805 nm and 829 nm. These spectra were efficiently converted to the mid IR, producing spectral power densities with the exact hole locations expected in the mid-IR at 2750 nm, 3000 nm, 3500 nm and 4000 nm (Fig.5(b)). This good correspondence between spectral profiles provides another verification of the main advantage of the adiabatic frequency conversion method, which is the separation between the seed spectral shape and the flat response of the nonlinear crystal, allowing the robust transfer of the spectral amplitude to another spectral range. Thus, a near-IR pulse shaper implemented prior to the conversion stage was used to shape the

spectrum of the generated mid-IR spectrum, thus demonstrating a highly convenient capability for multi-octave amplitude shaping.

5) **Pulse compression; Demonstration of a few-cycle, tunable mid-IR source.** [7]

By implementing a dispersion management system, including the acousto-optic programmable dispersive filter (AOPDF) prior to the conversion stage (See Fig. 2), and a highly efficient anti-reflection-coated bulk silicon block compressor after the conversion stage, we achieved tunable compressed mid-IR pulses spanning 2-4 microns with 4-cycle pulse durations. This first demonstration of compression of an ADFG source also confirmed that the spectral phase of the near-IR signal is transferred to the mid-IR idler, and the additional phase imparted by the adiabatic conversion process is smooth and easily removed using traditional dispersion management techniques.

We adjusted the dispersive properties of the AOPDF to pre-chirp the near-IR pulse such that after conversion to the mid-IR and propagation through the Si compressor the pulse would be fully compressed. Care was taken while choosing compressor length and AOPDF settings to maintain a good temporal overlap between interacting pulses in both the ADFG and second NOPA stages. The resulting compressed pulses were characterized in a homebuilt second-order interferometric autocorrelator, which uses either a 0.1-mm thick BBO crystal (for 2-μm operation) or a 0.4-mm thick AGS crystal (for 2.5-4.5-μm operation) for second harmonic generation (SHG), and an ext-InGaAs detector. The generated mid-IR spectrum can span from nearly 2-5 μm at -10 dB from peak, which supports a single-cycle pulse. However, the phase-matching bandwidth of the AGS autocorrelator crystal limited accurate autocorrelation measurements to ≥4-cycle pulses. Thus, we selected three narrower mid-IR spectral bands using the Dazzler to amplitude-shape the near-IR spectrum before conversion (Fig. 6(a,b)). The measured autocorrelation traces are plotted in Fig. 6(c-e), along with the expected autocorrelations assuming perfect SHG phase matching and a perfectly compressed (Fourier-limited) pulse. The transform limits of the measured spectra are 31 fs at 2.2 μm, 46 fs at 3.0 μm, and 49 fs at 3.7 μm, each ~4 optical cycles. The good match between the measured and expected autocorrelation traces shows there is an insignificant amount of spectral phase variation on the compressed mid-IR pulses. Thus, the pre-chirp imparted on the near-IR signal prior to conversion (experimentally optimized using the AOPDF by applying a quartic polynomial phase) compensated the spectral phase on the mid-IR pulse imparted by the adiabatic converter crystal and Si compressor. Note, an arbitrary phase could be added to the mid-IR pulse, if desired, by tuning the AOPDF.

DISTRIBUTION A: Distribution approved for public release.

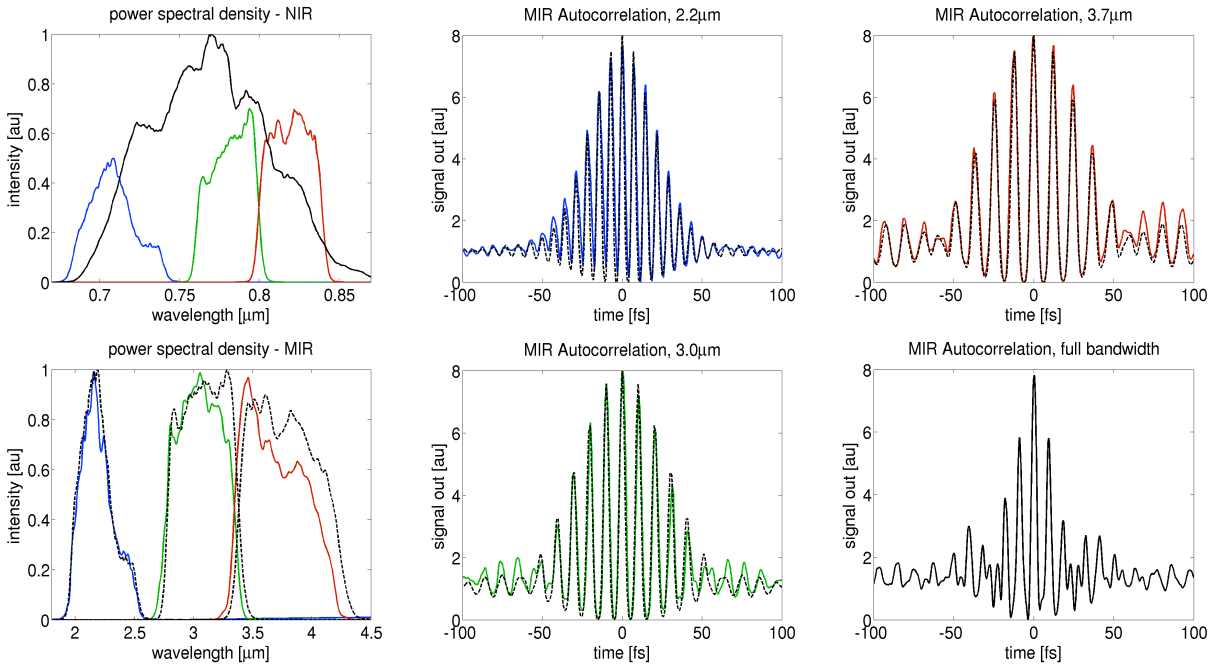

Fig. 6. (From [7]) Efficient and robust conversion of amplitude-shaped spectra. (a) Various OPCPA near-IR pulses that were shaped by an AOPDF in order to eliminate certain wavelength components in their spectral power densities. (b) The converted mid-IR spectra. As seen, one-to-one correspondence of the spectral hole locations and widths is achieved for all spectra.

6) **Modeling of propagation effects and parasitic processes.**

In order to achieve single-cycle, transform limited pulse durations, we needed to advance our understanding of the dispersion function of the ADFG process. Our first approach, using numerical propagation simulations, yielded a smooth phase function for passage through the adiabatic converter. Second, we derived an analytical formula for the dispersion function that was an excellent match to the results obtained numerically. This formula is linear, indicating that the ADFG device possesses a linear phase transfer function, a result that allows us to use the ADFG device, in tandem with a standard near-IR pulse shaper, as a multi-octave mid-IR pulse shaper. In the sections that follow, we show how both transform limited pulses and arbitrarily shaped octave-spanning mid-IR pulses can be obtained by use of the near-IR pulse shaper.

To model the temporal evolution of the mixing pulses throughout the adiabatic converter, we used a nonlinear propagation simulator based on the Fourier split-step method for solution of the coupled partial differential equations describing three-wave mixing in a dispersive medium with quadratic nonlinear susceptibility under the slowly varying envelope approximation. The numerical solver performed a (1+1)-D (longitudinal + temporal) simulation of the pulse using a temporal grid size of 2^{18} points and approximately 20,000 spatial steps, with pulses propagated in a retarded frame moving at the group velocity of the pump beam. For the linear step, the dispersion of the material is calculated directly from the Sellmeier coefficients, as given in Ref. [4]. In the nonlinear step, the nonlinear polarization fields describing sum- and difference-frequency generation by mixing of near-IR, mid-IR, and pump waves were numerically integrated using a 4^{th}-order Runge-Kutta algorithm, with the sign of the effective nonlinear coefficient flipped twice per ferroelectric domain poling period, $\Lambda_{QPM}(z)$, assuming a 50% duty-cycle with square edges. The ~1μm longitudinal step size ensured adequate sampling of the

QPM domains, which ranged from 4-12 μm throughout the crystal, as confirmed by negligible differences in the results when using smaller step sizes. The magnitude of the effective nonlinear coefficient d_{eff} was assumed to be 21.5 pm/V. Degenerate wave mixing (i.e., second harmonic generation and spontaneous downconversion), and all higher-order nonlinear processes (cubic and above) were ignored. Linear absorption in the MgO:CLN crystal was included, using the absorption data published in [8].

For a sufficiently long crystal (compared to the conversion length of the ADFG process), we found we could match the phase evolution solved by our propagation simulations with analytical formula for the group delay (GD) imparted on the final mid-IR field. This formula is comprised of two terms:

$$\tau(\omega) = k'(\omega + \omega_p) z_c(\omega) + k'(\omega)(L - z_c(\omega))$$

Where $k(\omega + \omega_p)$ and $k(\omega)$ are the near-IR and corresponding mid-IR wavenumbers, $k'(\omega)$ is $\partial k/\partial\omega$, $z_c(\omega)$ is the frequency dependent conversion position, and L is the length of the crystal. The first term represents the propagation of the near-IR field until it is converted at $z_c(\omega)$, while the second term represents propagation as a mid-IR field through the remaining length of the crystal. We can take successive derivatives to obtain higher order dispersion terms such as the group delay dispersion,

$$\tau'(\omega) = k''(\omega + \omega_p) z_c(\omega) + k''(\omega)\big(L - z_c(\omega)\big) + \Big(k'(\omega + \omega_p) - k'(\omega)\Big) z_c'(\omega),$$

where $k''(\omega)$ is $\partial k^2/\partial\omega^2$, and $z_c'(\omega)$ is $\partial z_c/\partial\omega$. We note the unusual final term that is a consequence of the frequency dependent conversion position.

We define the frequency dependent conversion position, $z_c(\omega)$, as the position of zero phase mismatch for each frequency ω. To calculate $z_c(\omega)$ we start by determining the QPM grating periods $\Lambda(\omega)$ for perfect phase matching, *i.e.*, such that $\Delta k_{eff}(\omega) = k(\omega + \omega_p) - k(\omega) - k(\omega_p) - \frac{2\pi}{\Lambda(\omega)} = 0$. By comparing $\Lambda(\omega)$ to the actual grating period of the crystal, we can determine the position of zero wavevector mismatch for each frequency ω, and, hence, the conversion position $z_c(\omega)$.

Given this definition of z_c, the physical interpretation of the accumulated GD is that a near-IR device of frequency dependent length $z_c(\omega)$ is followed by a mid-IR device of frequency dependent length $[L - z_c(\omega)]$, with instantaneous frequency conversion at the boundary point.

To test the validity of the analytical formula for $\tau(\omega)$ and the derived group delay dispersion (GDD) and third order dispersion (TOD), we compared these analytical quantities against the same quantities calculated by numerical solution of the coupled wave equations (as described above). Fig. 7 shows an excellent match between the simulated and analytic group delays between 1.6-6 μm, and very strong match for the GDD and TOD, with deviations beginning above 5 μm. Note, when plotting group delay we have subtracted off a constant (*i.e.*, wavelength independent) value for ease of comparison across the bandwidth.

DISTRIBUTION A: Distribution approved for public release.

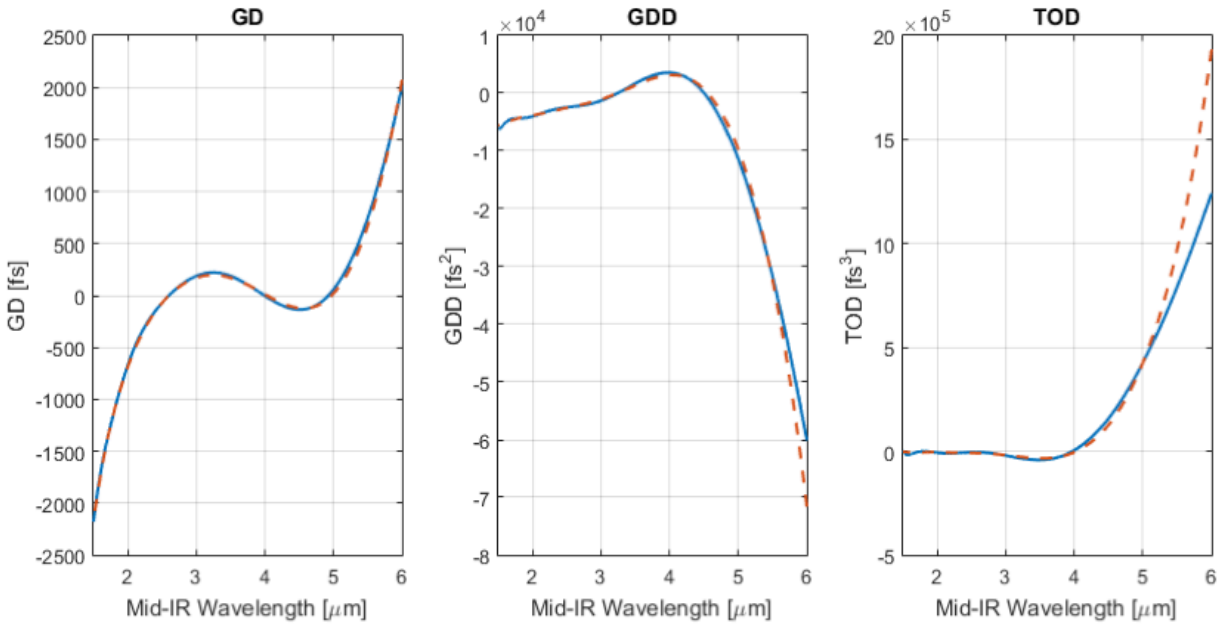

Fig. 7. : A comparison of the group delay (GD), group delay dispersion (GDD) and third-order dispersion (TOD) produced by the ADFG device as calculated from simulations (solid) and the analytic formula for the delay (dashed).

Thus, using this formula, a dispersion management system can be precisely designed. Moreover, it is evident that a properly designed adiabatic grating can be used to tailor the intrinsic dispersion profile of the device.

7) **Generation of single-cycle mid-IR pulses.** [9]

The fields of nonlinear infrared spectroscopy and strong-field laser-matter interaction call for intense and ever-shorter sources of mid-IR light, with many proposed experiments requiring greater-than-octave spanning bandwidths to be used for experiments requiring the shortest possible temporal resolution. Thus, it is highly desirable to be able to compress a multi-octave spectrum to its transform limit, which can correspond to a single optical cycle or less.

The temporal profile of the mid-IR pulse was characterized using frequency resolved optical gating (FROG) in a homebuilt autocorrelator. Noncollinear second harmonic generation in a 30 μm thick GaSe crystal (Eskma, GaSe-30H) was used as the nonlinear medium for FROG, and a grating spectrometer using an extended InGaAs linear array detector (Ocean Optics, NIR256) was used for the frequency resolved detector, with a 10 ms integration time. The retrieval was done using the code written by J. Wong and provided through the Trebino group, which implements the method of generalized projections [10]. As is the case for SHG-FROG, the retrieved direction of the pulse in time is ambiguous. All of the spectrometers were calibrated against a blackbody radiator (Electro Optical Industries, WS133) at 1280K.

The experimental setup is a slight modification of that in Fig. 2, and is shown below in Fig. 8. It consists of an octave-spanning Ti:Sapphire oscillator seed source, which is used to seed a 1 kHz Nd:YLF chirped pulse amplifier (CPA) system, and a 2-stage OPCPA system pumped by the same Nd:YLF amplifier. The OPCPA system uses 2 grism pairs and an AOPDF to chirp the near-IR pulses to an approximately 3 ps duration for efficient amplification by the second harmonic of the Nd:YLF laser. The resulting chirped near-IR pulses are downconverted to the

mid-IR using chirped pulse difference frequency generation with the narrowband 1047 nm output of the Nd:YLF amplifier using the ADFG crystal described in Section 1, to generate chirped pulses in the mid-IR. Finally, these are compressed in a 21-mm thick silicon block back to their transform limited duration.

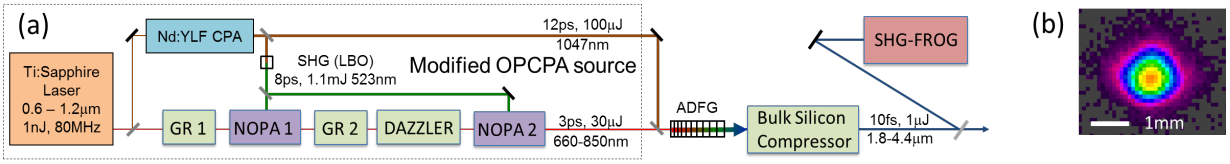

Fig. 8. (From [9]) (a) Experimental setup: Nd:YLF CPA, 12-ps, 1-kHz, 4-mJ; GR1, grism; NOPA1, BBO 5mm; GR2 grism; Dazzler (Fastlite); NOPA2, BBO 3mm; ADFG, aperiodically poled, 20-mm MgO-doped congruent $LiNbO_3$ grating; Compressor, Bulk Silicon Compressor, 21mm single pass. (b) Far field profile of compressed beam.

Due to the greater-than-octave spanning nature of the generated mid-IR pulse, the ability to arbitrarily shape its chirp through manipulation of the phase with a conventional near-IR pulse shaper is of critical importance to its compression. The near-IR pulse shaper was used to add a non-polynomial phase to fine-tune the chirp on the mid-IR pulse to exactly compensate for the dispersion mismatch between compressor, ADFG stage, and other dispersive optics in the system. The applied phase function for the full bandwidth of the pulse was determined by independently compressing 3 overlapping spectral bands (1.8-2.7 μm, 2.1-4.1 μm, and 3.5-4.4 μm), and then stitching the required spectral phase functions together to allow compression of the full pulse bandwidth (1.8-4.4 μm). To determine the correct phase function for compressing each individual band, a 4th-order polynomial phase was experimentally determined by iteratively applying a spectral phase using the pulse shaper and measuring the residual phase variation using FROG. The three individual phase functions were stitched together with care taken to ensure that the resulting full-bandwidth phase function was continuous and smooth up to its 2nd derivative.

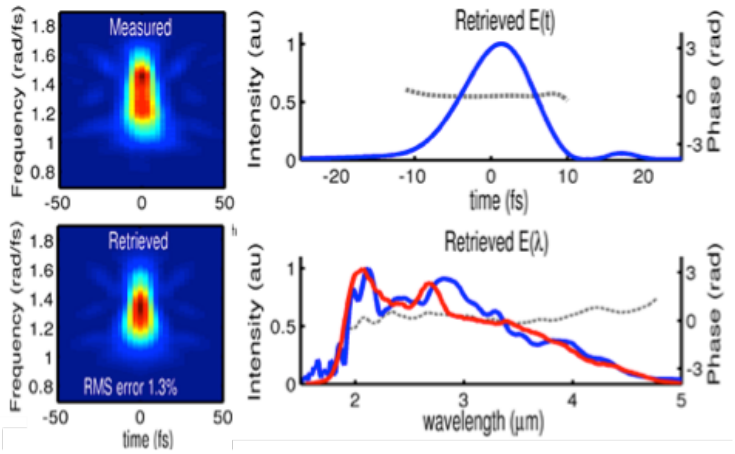

Fig. 9. (From [9]) Experimentally measured FROG characterization of compressed pulse: (a) Measured FROG trace. (b) Retrieved FROG trace. (c) Retrieved electric field in the temporal domain (blue: intensity, gray: phase). (d) Retrieved FROG trace in the spectral domain (blue: retrieved intensity, red: measured intensity; gray: phase).

The resulting compressed pulse is shown in Fig. 9. The compressed pulse has 1.5μJ energy and 11fs duration, which is 1.2 optical cycles at the central wavelength of 2.8 μm, and is within 15% of its transform-limited duration. We note that the arbitrary phase control afforded by the near-IR pulse shaper and the linear phase transfer function of the ADFG process makes pulse compression *in situ* possible, as it is possible to compensate for the dispersion of an experimental

setup (e.g., chamber windows, beamsplitters, gas through which the pulse propagates, etc.) that would otherwise be extremely challenging to remove using traditional pulse shaping techniques.

8) **Demonstration of arbitrary, multi-octave pulse shaping.** [11]

To date, octave-spanning sources of mid-IR light have not allowed pre-generation pulse shaping in order to arbitrarily control the resulting amplitude and phase. This is because many of the most successful technologies for octave-spanning mid-IR generation rely on self-phase modulation (*e.g.*, supercontinuum generation, filamentation, soliton compression, *etc.*), and thus the spectral broadening is inexorably tied to the temporal phase and amplitude evolution during generation. In these devices, arbitrary pulse shaping can only be achieved by a post-conversion pulse shaper, as arbitrary shaping prior to conversion would upset the desired nonlinear pulse evolution. The same limitation is true of common three-wave-mixing sources of mid-IR light such as optical parametric amplification (OPA) and difference frequency generation (DFG), in which the transfer functions for phase and amplitude are nonlinear in pulse intensity or require a temporally compressed driver pulse. Post-conversion shaping is a technically difficult proposition for octave-spanning bandwidths, as traditional pulse shapers based on spatial light modulators inside of grating pairs and acousto-optic programmable dispersive filters (AOPDF) have been limited to sub-octave-spanning bandwidths due to the second-order diffraction. And while extreme ultrashort pulse shaping through the modular control of distinct bands within a pulse synthesizer has become a reality in recent years [12], these devices grow more complex as spectral width is extended and have not yet covered the functional-group mid-IR range.

Making use of the property of linear phase transfer through the ADFG device and the property of increase in relative bandwidth through the near-IR to mid-IR conversion process, we can use our near-IR AOPDF prior to the ADFG device as, effectively, a multi-octave mid-IR pulse shaper. As a result, not only can we compress our multi-octave mid-IR pulses to their transform limit, but our results show that it is possible to transfer complex pulse profiles, thus demonstrating a clear route to multi-octave shaped mid-IR sources for spectroscopy and coherent control.

By tuning the AOPDF relative to the dispersion function that allowed transform-limited pulse compression, a variety of modulated pulses were generated and experimentally retrieved, as shown in Fig. 10. For illustration, 3 pulse shapes were selected. First, a simple linear chirp was applied to show that the pulse can be chirped to compensate for dispersive optical elements. Second, an interferometrically stable pulse pair was generated, as could be used in a multidimensional spectroscopy experiment. Finally, a sinusoidal phase modulation was applied to an otherwise transform limited pulse to add temporal sidebands, as might be done in a coherent control experiment. In all cases the spectral amplitude/phase of the retrieved pulse matched well with the applied amplitude/phase.

With this result, we have demonstrated arbitrary shaping of mid-IR bandwidths exceeding an octave, using adiabatic frequency conversion with chirped pulses. Our technique is the first that can produce simultaneously multi-octave spanning bandwidth, high-energy pulses, high conversion efficiency, and arbitrary pulse shaping. This unmatched capability paves the way for a new class of experiments in the mid-IR, in fields ranging from nonlinear vibrational spectroscopy to strong light-matter interaction physics and single-shot remote sensing.

DISTRIBUTION A: Distribution approved for public release.

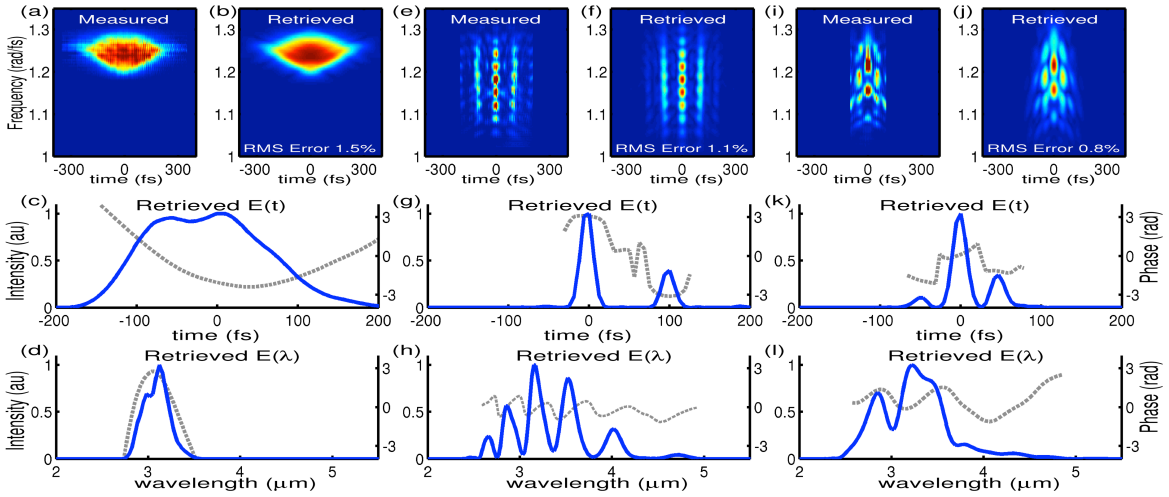

Fig. 10. (From [11]) Measured and Retrieved FROG traces (top row), retrieved electric field in the temporal domain (middle row; blue: intensity, gray: phase) and spectral domain (bottom row; blue:intensity, gray: phase), for 3 different input pulses. Left (a-d) linear chirp of 2000fs^2, middle(e-h) double pulse with 100fs separation, right (i-l) sinusoidal spectral phase modulation with amplitude of 1 radian and period of 2.00e13 Hz, corresponding to 100fs pulse separation between the generated pulses. Note-due to the low intensity of the chirped pulse in (a-d), the bandwidth of the pulse was narrowed to 500nm and a 400mm thick AGS crystal was used in the FROG.

9) **Implementation as a seed pulse for ultrabroadband mid-IR OPA.** [13]

We report on the demonstration of a mid-IR OPA centered at 6 μm, which uses ADFG pulses as a broadband, phase-controlled seed, and which is pumped by a 32 fs, 2.1-μm OPCPA. As our broadband 2-5 μm ADFG pulses can in the future be used in this type of OPA architecture both as the signal seed pulse and to seed powerful 2-μm Ho:YLF and Ho:YAG pump laser amplifiers, this OPA demonstration thus represents a route towards a simple ultrabroadband mid-wave IR amplifier system, with phase- and amplitude-controlled amplified pulses.

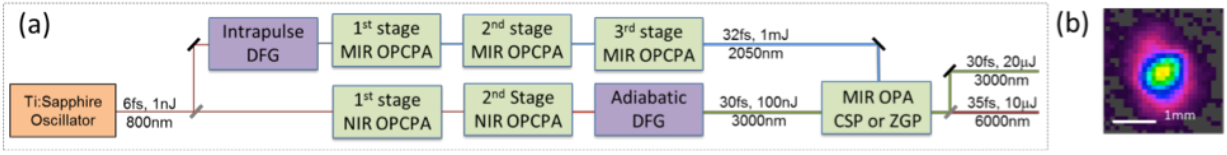

Fig. 11. (From [13]) (a) The schematic of the 6 μm mid-IR OPA (near-IR OPCPA pump lasers not shown for clarity). (b) The measured far field idler beam profile.

In this experiment, we report on the demonstration of a mid-IR optical parametric amplifier (OPA) generating an octave-spanning idler with central wavelength of 6.5 μm, energy of 10 μJ, and a pulse duration of approximately 35 fs, which operates at 1kHz. This amplifier is pumped by a 32 fs, 2.1 μm OPCPA, the construction of which is described in detail in [14], and seeded by a 30 fs, 3 μm sourced based on adiabatic difference frequency generation (ADFG), which is based on the source detailed in [1] with the bandwidth artificially narrowed to ~1 μm to match the gain bandwidth of the mid-IR OPA. The pump and seed beams were combined using a polarizing beam splitter (PBS) consisting of a silicon plate at Brewster's angle, and passed through the OPA crystal and amplified. The signal and idler were then separated using another silicon plate, and the idler was isolated from the signal using a 4.5 μm long-pass filter (LPF). The signal and idler spectra were measured using a scanning grating monochromator and the idler

was then characterized in a home built second order interferometric autocorrelator using an uncoated 1mm thick ZnSe plate as the beam splitter and a 30 μm thick GaSe crystal (z-cut) as the nonlinear medium. A mid-IR polarizer was used to block the residual fundamental wavelengths and a PbSe detector was used as a detector. We point out that the anomalous dispersion of the ZnSe beam splitter roughly compensates the normal dispersion of the LPF, however there is approximately 5000 fs^3 of residual uncompensated third order dispersion in this configuration. Two different crystals were explored for the OPA, a 0.5 mm thick ZGP crystal (type I, $\theta = 51°$) and a 1.1 mm thick CSP crystal (type I, $\theta = 45°$), both grown at BAE systems, and the performance of each material was independently evaluated. Neither crystal was anti-reflection coated, so there is a ~25% reflection from each surface.

Using 0.7 mJ pump energy (~350 GW/cm2) and 100 nJ seed energy (~50 MW/cm2) we observed an idler bandwidth spanning 4.5-9.0 μm, as shown in Fig. 12(a), and idler energy of 5.0 μJ (after accounting for 28% loss due to the uncoated silicon PBS). The measured idler beam profile is shown in Fig. 1(b), as observed on a pyroelectric camera. The measured interferometric autocorrelation trace is shown in Fig. 12(b), and is plotted with a simulated trace (calculated using the measured spectrum, and assuming a flat spectral phase); the good agreement between these pulses show that the idler is nearly compressed to its transform limited duration of 32 fs (1.5 optical cycles).

Using the 1.1 mm thick CSP crystal under the same conditions (0.7 mJ pump energy, 100 nJ seed energy) it was possible to produce an idler spanning 4.3-8.5 μm, with an idler energy of 10.1 μJ. However, the measured pulse duration in this configuration was significantly longer, as can be seen in the measured interferometric autocorrelation trace shown in Fig. 12(c) the pulse is significantly longer than its transform limited duration of 34 fs (1.6 optical cycles). This is partially due to additional dispersion from the thicker OPA crystal, however further investigation will be required to fully explain the discrepancy.

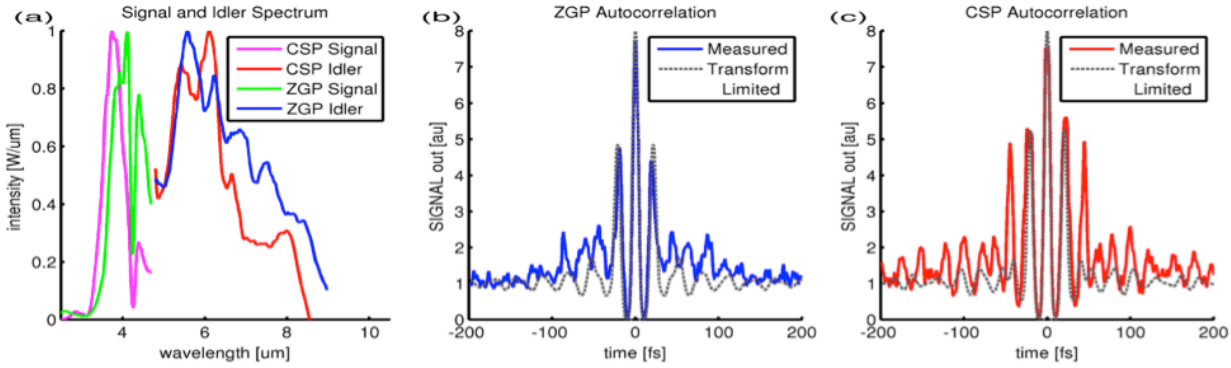

Fig. 12. (From [13]) (a)Measured amplified spectra of signal and idler with ZGP crystal and CSP crystal. (b) Measured autocorrelation of ZGP idler (blue) and transform limited autocorrelation (gray). (c) Measured autocorrelation of CSP idler (red) and transform limited autocorrelation (gray).

In conclusion, we have demonstrated a mid-IR OPA generating 1.5-optical-cycle pulses at 6.5 μm, with few-μJ energies at a 1 kHz repetition rate. The ultrabroadband idler generated spans nearly the entire mid-infrared spectral band from 4.5-9.0 μm, and has a peak power well in excess of 100 MW. This tunable, high-energy, few-cycle, mid-IR source is a useful tool for applications such as mid-IR spectroscopy, strong-field physics, and tissue ablation applications.

DISTRIBUTION A: Distribution approved for public release.

10) **Modeling and design of extended long-wave-IR source.**

The source achieved in this program, using aperiodically poled lithium niobate as the nonlinear medium, spans 60-160 THz (1.8-5 microns). This broad range thus bridges the wavelength gap between existing broadband near-infrared and terahertz sources. However, it would be highly desirable to further extend the bandwidth into the long-wave infrared. Employing our propagation simulations, we designed an extension of the frequency conversion technique to cover the thermal infrared along the 5-12 micron wavelength range (25-60 THz) using orientation poled gallium phosphide, to be used with a system design similar to that used for the lithium niobate device. The results (Fig. 13) show the possibility of obtaining the entire spectral range simultaneously, at ~50% photon number efficiency, from a single gallium phosphide grating. Continued research will determine whether such a source can be built.

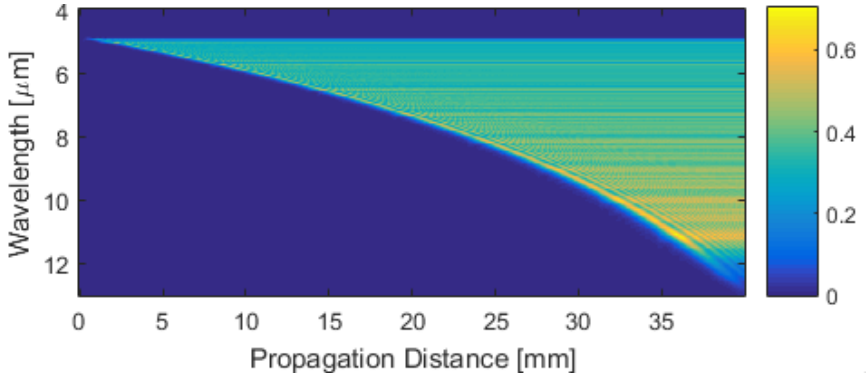

Fig. 13. Pulse propagation simulations of an ADFG device based on orientation patterned gallium phosphide. The pseudocolor scale indicates photon number conversion efficiency for the generated idler wavelengths. The broad transparency window of the device allows light to be generated up to 12 microns. In this example, ~50% conversion efficiency is predicted for all wavelengths in the range 5-12 microns.

11) **Design of multi-spectral, 10-fs spectroscopy system based on ADFG.**

We have developed a system architecture employing the ADFG approach in order to build a multi-spectral spectroscopy system at Cornell providing 10-fs pulses in many ranges of the electromagnetic spectrum. Using a picosecond, high-average power amplifier based on Yb:YAG and operating at 10 kHz, we generate a white-light-seeded few-cycle 800-nm OPCPA. This OPCPA system, also including near-IR pulse shapers, can be compressed and used as a near-IR pulse for spectroscopy, and/or used to drive several of three nonlinear frequency conversion stages, based on high harmonic generation (HHG) for EUV light generation, sum-frequency and second-harmonic generation for UV/Vis light generation, or ADFG for mid-IR generation. The 10-fs mid-IR pulse generation capability offered by the ADFG technology we have developed under this grant program extends the time resolution of such a multi-color spectroscopy source now also to 10-fs for mid-IR wavelengths. Moreover, using this design, these mid-IR pulses should be intense, phase-stable, and fully waveform controlled through the pulse shaper.

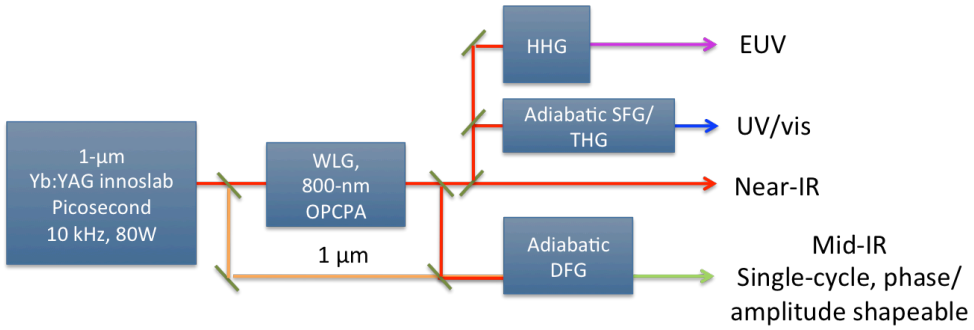

Fig. 14. Architecture for 10-fs multicolor nonlinear spectroscopy in development at Cornell University.

References

1. H. Suchowski, P. R. Krogen, S.-W. Huang, F. X. Kärtner, and J. Moses, "Octave-spanning coherent mid-IR generation via adiabatic difference frequency conversion," Opt. Express **21**, 28892 (2013).
2. J. Moses, H. Suchowski, and F. X. Kärtner, "Fully efficient adiabatic frequency conversion of broadband Ti:sapphire oscillator pulses," Opt. Lett. **37**, 1589–1591 (2012).
3. H. Suchowski, D. Oron, A. Arie, and Y. Silberberg, "Geometrical representation of sum frequency generation and adiabatic frequency conversion," Phys. Rev. A **78**, 63821 (2008).
4. O. Gayer, Z. Sacks, E. Galun, and A. Arie, "Temperature and wavelength dependent refractive index equations for MgO-doped congruent and stoichiometric LiNbO3," Appl. Phys. B **91**, 343–348 (2008).
5. I. Shoji, T. Kondo, A. Kitamoto, M. Shirane, and R. Ito, "Absolute scale of second-order nonlinear-optical coefficients," J. Opt. Soc. Am. B **14**, 2268 (1997).
6. J. Moses, S.-W. Huang, K.-H. Hong, O. D. Mücke, E. L. Falcao-Filho, A. Benedick, F. Ö. Ilday, A. Dergachev, J. A. Bolger, B. J. Eggleton, and F. X. Kärtner, "Highly stable ultrabroadband mid-IR optical parametric chirped-pulse amplifier optimized for superfluorescence suppression," Opt. Lett. **34**, 1639–1641 (2009).
7. P. R. Krogen, H. Suchowski, G. J. Stein, F. X. Kärtner, and J. Moses, "Tunable Few-Cycle Mid-IR Pulses towards Single-Cycle Duration by Adiabatic Frequency Conversion," in *19th International Conference on Ultrafast Phenomena*, OSA Technical Digest (Online) (Optical Society of America, 2014), p. 08.Tue.D.6.
8. L. E. Myers and W. R. Bosenberg, "Periodically poled lithium niobate and quasi-phase-matched optical parametric oscillators," IEEE J. Quantum Electron. **33**, 1663–1672 (1997).
9. P. Krogen, H. Suchowski, H. Liang, K.-H. Hong, F. Kaertner, and J. Moses, "Generation of a Single-Cycle Pulse at 2.6 µm using Adiabatic Difference Frequency Generation," in (OSA, 2016), p. UTu2A.1.
10. R. Trebino, K. W. DeLong, D. N. Fittinghoff, J. N. Sweetser, M. A. Krumbügel, B. A. Richman, and D. J. Kane, "Measuring ultrashort laser pulses in the time-frequency domain using frequency-resolved optical gating," Rev. Sci. Instrum. **68**, 3277–3295 (1997).
11. P. Krogen, H. Suchowski, H. Liang, F. X. Kaertner, and J. Moses, "Toward Multi-Octave Pulse Shaping by Adiabatic Frequency Conversion," in (OSA, 2015), p. SW1O.3.
12. C. Manzoni, O. D. Mücke, G. Cirmi, S. Fang, J. Moses, S.-W. Huang, K.-H. Hong, G. Cerullo, and F. X. Kärtner, "Coherent pulse synthesis: towards sub-cycle optical waveforms," Laser Photonics Rev. **9**, 129–171 (2015).

DISTRIBUTION A: Distribution approved for public release.

13. P. Krogen, H. Liang, K. T. Zawilski, P. G. Schunemann, T. Lang, U. Morgner, J. A. Moses, F. X. Kaertner, and K.-H. Hong, "Octave-spanning 1.5-optical-cycle 6.5-μm OPA pumped by 2.1-μm OPCPA," in (OSA, 2016), p. STu3I.4.
14. K.-H. Hong, C.-J. Lai, J. P. Siqueira, P. Krogen, J. Moses, C.-L. Chang, G. J. Stein, L. E. Zapata, and F. X. Kärtner, "Multi-mJ, kHz, 21 μm optical parametric chirped-pulse amplifier and high-flux soft x-ray high-harmonic generation," Opt. Lett. **39**, 3145 (2014).

DISTRIBUTION A: Distribution approved for public release.

AFOSR Deliverables Submission Survey

Response ID:7118 Data

1.

Report Type

Final Report

Primary Contact Email

Contact email if there is a problem with the report.

moses@cornell.edu

Primary Contact Phone Number

Contact phone number if there is a problem with the report

607-255-6704

Organization / Institution name

Cornell University/MIT

Grant/Contract Title

The full title of the funded effort.

(YIP) High-Energy, Multi-Octave-Spanning Mid-IR Sources via Adiabatic Difference Frequency Generation

Grant/Contract Number

AFOSR assigned control number. It must begin with "FA9550" or "F49620" or "FA2386".

FA9550-13-1-0159

Principal Investigator Name

The full name of the principal investigator on the grant or contract.

Jeffrey Moses/Franz X. Kaertner

Program Officer

The AFOSR Program Officer currently assigned to the award

Enrique Parra

Reporting Period Start Date

03/15/2013

Reporting Period End Date

07/14/2016

Abstract

The creation of energetic, arbitrarily shapeable, multi-octave-spanning, coherent sources of short-wave, mid-wave, and long-wave mid-IR light is valuable to many independent fields of research and technology development, from detection of ultrafast energy transfer in proteins and biological molecules across functional groups, to high-flux, table-top generation of coherent keV photons, time-resolved tomography of molecular orbital structure, and coherent control of vibrational dynamics of molecules. And it could further applications as diverse as laser ablation of polymers, infrared countermeasures for defense, laser ranging, and compact electron beam acceleration.

Under this grant, we have achieved the main goals of our research plan. We have evaluated a brand-new concept in nonlinear optics, adiabatic difference frequency generation (ADFG) for the efficient transfer of broadband, high-energy near-IR lasers to the mid-IR, allowing the generation of high-energy, multi-octave-spanning, short- and mid-wave IR pulsed sources in the 2-5 μm range and demonstration of compressed single-cycle mid-IR pulses. Adiabatic frequency conversion applies the concept of robust population transfer by rapid adiabatic passage to nonlinear optical frequency conversion. The concept effectively

avoids two main hurdles of optical frequency generation: limited bandwidth and limited conversion efficiency.

Moreover, we have shown that our ADFG technique is particularly convenient for the low-cost extension to the mid-IR of existing ultrafast laser architectures in the near-IR, requiring the addition of only a single nonlinear conversion stage based on an aperiodically poled quasi-phase-matching grating. Thus, a broadband source built on conventional laser technology can be immediately extended to the mid-IR, thus saving a research facility the considerable expense of a new laser system built to span a mid-IR frequency range. In our work, we have shown how the addition of a single adiabatic conversion stage to a conventional noncollinear, near-IR optical parametric chirped pulse amplification (OPCPA) system, can produce a multi-octave spanning mid-IR source emitting single-cycle and arbitrarily shaped mid-IR pulses. Additionally, we have shown that the ADFG mid-IR pulses can be used conveniently as the seed source for an octave-spanning mid-IR OPCPA pumped by 2-micron wavelength pulses.
Furthermore, we have experimentally verified that ADFG transfers the spectral phase and amplitude profile of the near-IR pulse to the mid-IR pulse with a linear transfer function, and its conversion efficiency does not depend on the initial phase and amplitude of the near-IR pulse. This "one-to-one" conversion dynamic allows a pulse to be modulated in the near-IR by existing pulse-shaping techniques, and desired phase and amplitude properties of the octave-spanning mid-IR pulse can be obtained without the photon losses or dollar costs for shaping technologies in the mid-IR spectral range.

Importantly, this means that the ADFG approach, including a conventional sub-octave near-IR pulse shaper (such as an acousto-optic programmable dispersive filter (AOPDF) or 4f-pulse shaper), can be used as a multi-octave mid-IR pulse shaper. We have demonstrated such a technology for the first time.

Finally, we advanced the approach towards future directions. Through modeling of ultrabroadband ADFG pulse propagation we have identified an analytical formula capturing the dispersion of the ADFG device. We have evaluated and modeled the extension of the ADFG approach to the long-wave IR through the use of orientation patterned semiconductors. And we have developed a scheme for employing the ADFG approach in a multi-spectral spectroscopy system providing 10-fs pulses in many ranges of the electromagnetic spectrum.

Distribution Statement

This is block 12 on the SF298 form.

Distribution A - Approved for Public Release

Explanation for Distribution Statement

If this is not approved for public release, please provide a short explanation. E.g., contains proprietary information.

SF298 Form

Please attach your SF298 form. A blank SF298 can be found here. Please do not password protect or secure the PDF The maximum file size for an SF298 is 50MB.

sf0298.pdf

Upload the Report Document. File must be a PDF. Please do not password protect or secure the PDF . The maximum file size for the Report Document is 50MB.

FA9550-13-1-0159 Final Report.PDF

Upload a Report Document, if any. The maximum file size for the Report Document is 50MB.

Archival Publications (published) during reporting period:

1. H. Suchowski, P. R. Krogen, S.-W. Huang, F. X. Kärtner, and J. Moses, "Octave-spanning coherent mid-IR generation via adiabatic difference frequency conversion," Opt. Express 21, 28892-28901 (2013).

2. K.-H. Hong, C.-J. Lai, J. Siqueira, P. Krogen, J. Moses, L. C.-L. Chang, G. J. Stein, L. E. Zapata, and F. X. Kärtner "Multi-mJ, kHz, 2.1-µm optical parametric chirped-pulse amplifier and high-flux soft X-ray high-harmonic generation," Opt. Lett. 39, 3145 (2014).

3. C. Manzoni, O. D. Mücke, G. Cirmi, S. Fang, J. Moses, S.-W. Huang, K.-H. Hong, G. Cerullo, and F. X. Kärtner, "Coherent pulse synthesis: towards sub-cycle optical waveforms," Laser & Photon. Rev. 9, 129 (2015).

4. C.-L. Chang, P. Krogen, H. Liang, G. J. Stein, J. Moses, C.-J. Lai, J. P. Siqueira, L. E. Zapata, F. X. Kärtner, and K.-H. Hong, "Multi-mJ, kHz, ps deep-ultraviolet source," Opt. Lett. 40, 665 (2015).

5. C.-L. Chang, P. Krogen, K.-H. Hong, L. E. Zapata, J. Moses, A.-L. Calendron, H. Liang, C.-J. Lai, G. J. Stein, P. D. Keathley, G. Laurent, and F. X. Kärtner, "High-energy, kHz, picosecond hybrid Yb-doped chirped-pulse amplifier," Opt. Express 23, 10132 (2015).

6. C.-J. Lai, K.-H. Hong, J. P. Siqueira, P. Krogen, C.-L. Chang, G. J. Stein, H. Liang, P. D. Keathley, G. Laurent, J. Moses, L. E. Zapata, and F. X. Kärtner, "Multi-mJ mid-infrared kHz OPCPA and Yb-doped pump lasers for tabletop coherent soft x-ray generation," J. Opt. 17, 094009 (2015).

7. C. Manzoni, O. D. Mücke, G. Cirmi, S. Fang, J. Moses, S.-W. Huang, K.-H. Hong, G. Cerullo, and F. X. Kärtner, "Coherent pulse synthesis: towards sub-cycle optical waveforms," Laser & Photon. Rev. 9, 129 (2015).

Conference papers during the reporting period, not yet published in archival journals:

1. P. Krogen, H. Suchowski, G. J. Stein, F. Kärtner, and J. Moses, "Tunable and Near-Fourier-limited Few-Cycle Mid-IR Pulses via an Adiabatically Chirped Difference Frequency Grating," in CLEO: 2014, OSA Technical Digest (online) (Optical Society of America, 2014), paper SM3I.5.

2. P. R. Krogen, H. Suchowski, G. J. Stein, F. X. Kärtner, and J. Moses, "Tunable Few-Cycle Mid-IR Pulses towards Single-Cycle Duration by Adiabatic Frequency Conversion," in 19th International Conference on Ultrafast Phenomena, OSA Technical Digest (online) (Optical Society of America, 2014), paper 08.Tue.D.6.

3. P. Krogen, H. Suchowski, H. Liang, F. X. Kaertner, and J. Moses, "Toward Multi-Octave Pulse Shaping by Adiabatic Frequency Conversion," in CLEO: 2015, OSA Technical Digest (online) (Optical Society of America, 2015), paper SW1O.3.

4. P. Krogen, H. Suchowski, H. Liang, K.-H. Hong, F. Kärtner, J. Moses, "Generation of a Single-Cycle Pulse at 2.6 μm using Adiabatic Difference Frequency Generation," in International Conference on Ultrafast Phenomena, OSA Technical Digest (online) (Optical Society of America, 2016), paper UTu2A.1.

5. H. K. Liang, P. Krogen, K. Zawilski, P. G. Schunemann, T. Lang, U. Morgner, F. Kärtner, J. Moses, and K. Hong, "Octave-Spanning 6-μm OPA Pumped by 2.1-μm OPCPA," in High-Brightness Sources and Light-Driven Interactions, OSA technical Digest (online) (Optical Society of America, 2016), paper MS4C.1.

6. P. Krogen, H. K. Liang, K. Zawilski, P. G. Schunemann, T. Lang, U. Morgner, J. Moses, F. Kärtner, and K. Hong, "Octave-spanning 1.5-optical-cycle 6.5-μm OPA pumped by 2.1-μm OPCPA," in Conference on Lasers and Electro-Optics, OSA Technical Digest (2016) (Optical Society of America, 2016), paper STu3I.4.

New discoveries, inventions, or patent disclosures:
Do you have any discoveries, inventions, or patent disclosures to report for this period?

No

Please describe and include any notable dates

Do you plan to pursue a claim for personal or organizational intellectual property?

Changes in research objectives (if any):

Change in AFOSR Program Officer, if any:

Extensions granted or milestones slipped, if any:

4-month no cost extension granted, extending period of performance to July 14, 2016.

AFOSR LRIR Number

LRIR Title

Reporting Period

Laboratory Task Manager

Program Officer

Research Objectives

Technical Summary

Funding Summary by Cost Category (by FY, $K)

	Starting FY	FY+1	FY+2
Salary			
Equipment/Facilities			
Supplies			
Total			

Report Document

Report Document - Text Analysis

Report Document - Text Analysis

Appendix Documents

2. Thank You

E-mail user

Oct 14, 2016 11:26:58 Success: Email Sent to: moses@cornell.edu

DISTRIBUTION A: Distribution approved for public release.